Recoil-induced resonances in pump-probe spectroscopy

P. R. Berman and B. Dubetsky
Physics Department, Randall Laboratories, University of Michigan, Ann Arbor, Michigan 48109-1120

J. Guo
Joint Institute for Laboratory Astrophysics, University of Colorado, Boulder, Colorado 80309-0440

(Received 27 December 1994)

When a pump field and probe field simultaneously drive an electronic-state atomic transition, the probe field absorption spectrum can consist of an absorption peak centered near $\Delta'=0$ and amplification peak centered near $\Delta'=2\Delta$ (Δ and Δ' are the pump and probe field detunings from the atomic transition frequency, respectively). This type of spectrum is seen in the limit $|\Delta| \gg \chi \gg \Gamma$, where χ is the Rabi frequency associated with the pump field and 2Γ is the homogeneous width associated with the atomic transition. For atoms cooled below the recoil limit of laser cooling, the qualitative nature of the probe absorption spectrum can undergo a dramatic change. Provided that the recoil splitting ω_k is larger than the homogeneous decay rate (as might occur in the case of a forbidden transition), the absorption and amplification features *each* split into an absorption-amplification doublet. In addition, structure is found in the probe absorption spectrum near $\Delta'=\Delta$; this structure consists of two absorption-amplification doublets. Both doublets can be resolved if $\omega_k > \Gamma$. If $\omega_k < \Gamma$, one of the doublets can be resolved provided that $\omega_k > \Gamma_A$, where Γ_A is some effective atomic ground state width in the problem. The positions, widths, and relative weights of all the components are readily predicted using a dressed-atom theory in which quantization of the center-of-mass momentum is included. An analytical expression for the probe field spectrum is obtained for a simple case in which spontaneous decay to the lower level is neglected. Validity criteria for the results are discussed.

PACS number(s): 32.80.Pj, 32.70.Jz, 42.50.−p

I. INTRODUCTION

When the absorption of a weak probe field is monitored as a function of its detuning from an atomic transition frequency, one obtains a spectrum that characterizes the linear absorption of the probe field by the medium. If a pump field of arbitrary intensity simultaneously drives the atomic transition, the probe absorption spectrum can undergo a qualitative change. The modification of the probe absorption spectrum depends on factors such as the pump-field intensity and detuning from resonance, the relative propagation directions of the pump and probe fields, the Doppler widths associated with the various processes that are occurring, and the decay rates associated with the atomic state populations and coherences.

For atom-field detunings that are greater than the homogeneous decay rate of the atomic-state coherence, the probe absorption spectrum has the general form shown in Fig. 1 [1]. In drawing Fig. 1, we have neglected any contributions to the line shape arising from the Doppler effect. Experimentally, Doppler shifts can be suppressed by using an atomic beam and laser fields that propagate perpendicular to the beam; in this manner, an absorption spectrum of the type shown in Fig. 1 has been observed [2]. Another method for reducing or eliminating the line-shape modifications arising from the Dopper effect is to cool the atoms using laser-cooling techniques. The absorption features at $\delta=-\Delta$ and gain feature at $\delta=\Delta$ (δ is the difference between probe and pump field frequencies and Δ is the pump field detuning from resonance) are conveniently explained in terms of a dressed atom picture [3]. In Fig. 1, a dispersionlike "nonsecular" contribution to the line shape, centered near $\delta=0$, has

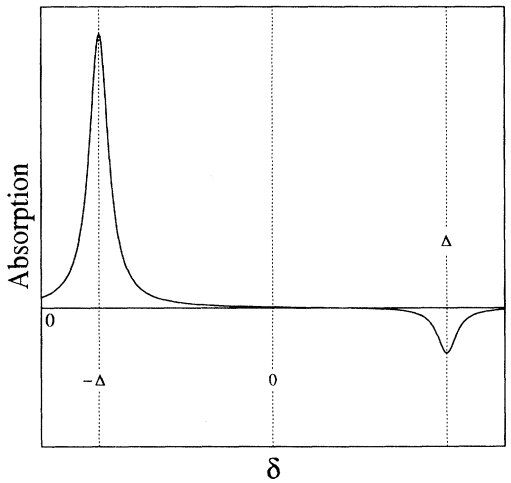

FIG. 1. A typical probe absorption line shape, neglecting any effects of Doppler broadening. Probe absorption is plotted as a function of the frequency difference δ between the probe and pump beams. In addition to the absorption component centered at $\delta=-\Delta$, there is a "Raman-like" gain component centered at $\delta=\Delta$ (Δ is the detuning of the pump field from the atomic transition frequency). The spectrum is drawn in the limit that $\Delta \gg \chi \gg \Gamma$, where χ is the pump-field Rabi frequency. The amplitude of the gain component at $\delta=\Delta$ is not drawn to scale; in reality it is $|\chi/\Delta|^4$ times smaller than the absorption peak.

not been included. For a fixed ratio of the pump field Rabi frequency χ to detuning Δ, the nonsecular contribution vanishes in the limit $|\Delta|/\Gamma \sim \infty$, where Γ is the homogeneous half-width at half maximum (HWHM) associated with the transition. In the following discussion, we neglect any such nonsecular terms.

The purpose of this paper is to examine modifications to the probe absorption profile resulting from atomic recoil on the absorption or emission of radiation. The possibility of measuring a recoil splitting using nonlinear optical spectroscopy was proposed by Kol'chenko, Rautian, and Sokolovskii [4] and observed experimentally using saturation spectroscopy [5], Ramsey fringes [6], and two-quantum transitions [7]. We have shown previously [8] that inclusion of recoil effects can lead to new structure in the probe absorption spectrum centered near $\delta=0$. Such recoil-induced resonances (RIR) have been observed experimentally [9] and have been used to probe the velocity distribution of a laser-cooled vapor [10]. The original theory of the RIR [8] has been generalized to include effects related to magnetic state degeneracy and localization of the atoms in the optical potentials [11]. Theories of RIR applicable to the transient domain have also appeared [12,13]. Although the theories generally put no restriction on the ratio

$$r=2mu/\hbar|\mathbf{k}-\mathbf{k}'| \tag{1}$$

of the residual Doppler width $|\mathbf{k}-\mathbf{k}'|u$ to recoil shift $\hbar|\mathbf{k}-\mathbf{k}'|^2/2m$ ($\mathbf{k}$ and $\mathbf{k}'$ are the pump and probe field propagation vectors, respectively, u is the most probable atomic speed, and m is the atomic mass), theory and experiment (with the exception of Ref.[13]) have concentrated on limits in which $r \gg 1$.

In this paper, we consider a subrecoil limit of laser cooling in which $r<1$, or

$$k_B T \ll \hbar\omega_k, \hbar|\mathbf{k}-\mathbf{k}'|^2/2m \ , \tag{2}$$

where $T=mu^2/2k_B$ is a temperature associated with the vapor and $\omega_k=\hbar k^2/2m$ is a recoil frequency. In the subrecoil limit, the pump-probe spectrum can contain up to eight components (see Fig. 2) having positions, widths, and amplitudes that depend on field strength, detunings, relaxation rates, and recoil frequency. We refer to these features of the spectrum as Stark-recoil components (SRC's) since they are related to both recoil and Stark splitting of the lines. Several schemes have been proposed [14] to cool neutral atoms below the recoil limit; experimental observations of subrecoil cooling have been reported [15].

It should be noted that theories of recoil splitting in saturation spectroscopy can be written in a form that implicitly incorporates several of the features of pump-probe spectroscopy. This is most clearly evident in the paper of Stenholm [16], who considers the probe absorption of a field having a frequency equal to that of a counterpropagating pump field. For atoms having a given projection of atomic velocity v along the direction of the pump field propagation vector $\mathbf{k}$, the difference in frequency between the probe and pump field frequencies in the atomic rest frame is $\bar{\delta}=2kv$. A graph of probe absorption versus kv can then mirror a probe absorption spectrum if the substitution $kv \leftrightarrow \delta/2$ is made. A direct comparison with Stenholms' result is not transparent, however, since he considers a flat velocity distribution and translates the central positions of some of the resonances by amounts of order of the recoil splitting. As such, the resonances centered near $\delta=0$ (for which he obtains a splitting into two dispersionlike components) actually represent nonsecular terms in his theory; in addition he does not obtain the B_1 or B_2 resonances shown in Fig. 2.

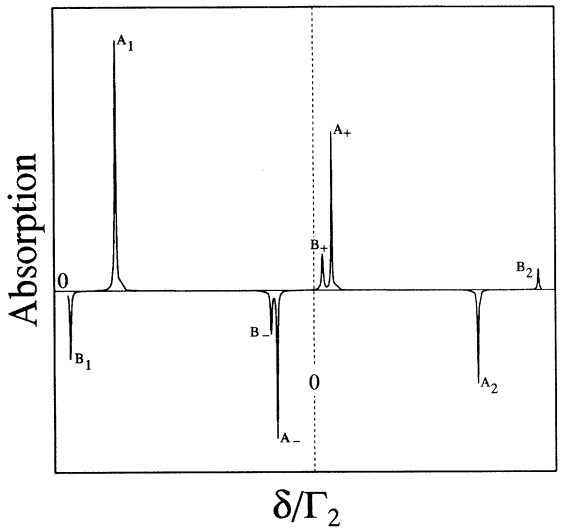

FIG. 2. Probe absorption versus dimensionless detuning δ/Γ_2 (Γ_2 is the upper state decay rate), with the inclusion of recoil. The pump detuning is $\Delta/\Gamma_2=50$, pump field Rabi frequency $\chi/\Gamma_2=75$, the recoil frequency is $\omega_k/\Gamma_2=5$, and $\Gamma_1/\Gamma_2=0.05$.

This paper is arranged as follows. In Sec. II, the dressed-atom states are constructed, taking into account quantization of the atomic center-of-mass motion. The different SRCs and their positions are readily determined in this dressed atom picture. In Sec. III the dressed-atom representation is also used to obtain the SRC line shape. An analytical expression for the SRC line shape, not restricted to the secular approximation, is obtained in Sec. IV using a model in which radiative decay between the transition levels is neglected. The limits of validity of the model are discussed in Sec. V, and a discussion of the physical origin of the various spectral components in terms of a bare-state picture is also presented.

II. DRESSED-STATE ENERGIES INCLUDING QUANTIZATION OF THE ATOMIC CENTER-OF-MASS MOMENTUM

Consider a two-level atom in a strong pump field propagating along the x axis. In the resonance or rotating-wave approximation, the interaction Hamiltonian for the atom-field system can be written as

$$V=\hbar[gS^{\dagger}ae^{ikx}+g^{*}Sa^{\dagger}e^{-ikx}] \ , \tag{3}$$

where $S=|1\rangle\langle 2|$, $|1\rangle$ and $|2\rangle$ are the lower and upper

atomic states, respectively, $\mathbf{k}=k\hat{\mathbf{x}}$ is the photon wave vector, a and $a^\dagger$ are creation and destruction operators for mode $\mathbf{k}$, and g is a coupling coefficient. Bare states of the atom-field system are denoted by $|i,n,p\rangle$, where i labels an internal state of the atom, n is the number of pump photons, and p is the atomic momentum in the x direction. The Hamiltonian (3) couples states $|1,n,p\rangle$ and $|2,n-1,p+\hbar k\rangle$.

From the Schrödinger equation $H|\rangle=E|\rangle$, where $H=H_0+V$ and $H_0=p^2/2m+\hbar\omega|2\rangle\langle 2|+\hbar\Omega a^\dagger a$, one arrives at a secular equation for dressed-state energies given by

$$\begin{vmatrix} \epsilon_p-E & \hbar\chi^* \\ \hbar\chi & \epsilon_{p+\hbar k}-\hbar\Delta-E \end{vmatrix}=0 , \tag{4}$$

where

$$\epsilon_p=p^2/2m \tag{5}$$

is the center-of-mass kinetic energy, $\chi=\sqrt{n}g$ is a Rabi frequency, and $\Delta=\Omega-\omega$ is the detuning of the pump field from the $2\rightarrow 1$ transition frequency ω. The energy of the bare state $|1,n,p=0\rangle$ has been set equal to zero, and it is assumed that $n\gg 1$. From Eq. (4), one finds the energies of the dressed states to be

$$E_{A,B}=\epsilon_p+\tfrac{1}{2}\hbar\{-\tilde{\Delta}+\omega_k\pm[(\tilde{\Delta}-\omega_k)^2+4|\chi|^2]^{1/2}\} , \tag{6}$$

where $\tilde{\Delta}=\Delta-kv$, and $v=p/m$ is the x component of the atomic velocity.

To further simplify the calculations, we assume that the recoil frequency is smaller than the detuning or Rabi frequency

$$\omega_k\ll\max(|\chi|,|\tilde{\Delta}|) . \tag{7}$$

In this limit, Eq. (6) reduces to

$$E_{A,B}=\epsilon_p+\tfrac{1}{2}\hbar[\pm\omega_{AB}-\tilde{\Delta}+\omega_k(1\mp\tilde{\Delta}/\omega_{AB})] , \tag{8a}$$

where

$$\omega_{AB}=(\tilde{\Delta}^2+4|\chi|^2)^{1/2} . \tag{8b}$$

To zeroth order in ω_k, the eigenvectors corresponding to the energies (8a) are given by

$$|A(n,p)\rangle=\cos(\theta)|1,n,p\rangle+\sin(\theta)|2,n-1,p+\hbar k\rangle , \tag{9a}$$

$$|B(n,p)\rangle=-\sin(\theta)|1,n,p\rangle+\cos(\theta)|2,n-1,p+\hbar k\rangle , \tag{9b}$$

$$\cos(\theta)=[(\omega_{AB}+\tilde{\Delta})/2\omega_{AB}]^{1/2} , \tag{9c}$$

where $0\le\theta\le\pi/2$. The states are defined such that $E_A>E_B$. Moreover for $\tilde{\Delta}>0$, $\theta\sim 0$ as $\chi\sim 0$. For the sake of definiteness, we choose $\tilde{\Delta}>0$, which further limits θ to the range $0\le\theta\le\pi/4$. In the Appendix, condition (7) is relaxed and expressions are derived for the SRC amplitudes, widths, and positions valid for arbitrary ratios of ω_k to ω_{AB}.

The probe field, having wave vector $\mathbf{k}'=-\mathbf{k}$ and frequency Ω', drives transitions between dressed states differing in both photon number and momentum. In the spirit of other dressed-atom treatments [3], we do not quantize the probe field. Nevertheless, we must account for the change in momentum of the atom on absorption or emission of a probe photon. Probe absorption occurs between states $|1,n,p\rangle$ and $|2,n,p+\hbar k'\rangle$ which is equivalent to coupling the $\{n,p\}$ and $\{n+1,p+\hbar(k'-k)\}$ dressed-state manifolds. Probe emission occurs between states $|2,n-1,p+\hbar k\rangle$ and $|1,n-1,p+\hbar(k-k')\rangle$, which is equivalent to coupling the $\{n,p\}$ and $\{n-1,p+\hbar(k-k')\}$ manifolds. The relevant eigenstates and energy levels are shown in Figs. 3(a) and 3(b), respectively. It is now a relatively simple matter to determine the positions of the various absorption and emission components using Eq. (8) [and Fig. 3(b)]. We can separate the resonances into three regions. The individual resonances are identified in Fig. 3(c).

Absorption from $|A(n,p)\rangle$ to $|B(n+1,p+\hbar(k'-k))\rangle$ is resonant at

$$\tilde{\delta}_{A_1}=-\omega_{AB}+\omega_k[1+2\sin^2(\theta)] , \tag{10}$$

while emission from $|B(n,p)\rangle$ to $|A(n-1,p+\hbar(k-k'))\rangle$ is resonant at

$$\tilde{\delta}_{B_1}=-\omega_{AB}-3\omega_k[1+2\sin^2(\theta)] , \tag{11}$$

where $\tilde{\delta}=\delta+2kv$. In the absence of recoil, both resonances, labeled A_1 and B_1, are centered at $\tilde{\delta}=-\omega_{AB}$, reproducing the absorption peak shown in Fig. 1.

Emission from $|A(n,p)\rangle$ to $|B(n-1,p+\hbar(k-k'))\rangle$ is resonant at

$$\tilde{\delta}_{A_2}=\omega_{AB}-3\omega_k[3-2\sin^2(\theta)] , \tag{12}$$

while absorption from $|B(n,p)\rangle$ to $|A(n+1,p+\hbar(k'-k))\rangle$ is resonant at

$$\tilde{\delta}_{B_2}=\omega_{AB}+\omega_k[3-2\sin^2(\theta)] . \tag{13}$$

In the absence of recoil, both resonances, labeled A_2 and B_2, are centered at $\delta=\omega_{AB}$, reproducing the "Raman" emission peak shown in Fig. 1.

Absorption from $|A(n,p)\rangle$ to $|A(n+1,p+\hbar(k'-k))\rangle$ is resonant at

$$\tilde{\delta}_{A_+}=4\omega_k\cos^2(\theta) , \tag{14}$$

while emission from $|A(n,p)\rangle$ to $|A(n-1,p+\hbar(k-k'))\rangle$ is resonant at

$$\tilde{\delta}_{A_-}=-4\omega_k[1+\sin^2(\theta)] . \tag{15}$$

In the absence of recoil, both resonances, labeled $A_\pm$ are centered at $\tilde{\delta}=0$, canceling each other in the secular approximation. If ω_k is nonvanishing but small ($\omega_k\ll|\mathbf{k}'-\mathbf{k}|u$), these resonances correspond to the RIR discussed in earlier published works [8–12].

Absorption from $|B(n,p)\rangle$ to $|B(n+1,p+\hbar(k'-k))\rangle$ is resonant at

$$\tilde{\delta}_{B_+}=4\omega_k\sin^2(\theta) , \tag{16}$$

while emission from $|B(n,p)\rangle$ to $|B(n-1,p$

$+\hbar(k-k'))\rangle$ is resonant at

$$\tilde{\delta}_{B_-} = -4\omega_k[1+\cos^2(\theta)] \ . \tag{17}$$

In the absence of recoil, both resonances, labeled $B_\pm$, are centered at $\tilde{\delta}=0$, canceling each other in the secular approximation.

III. SRC LINE SHAPE

The widths and relative weights of the resonances depend on the various relaxation rates and the width of the velocity distribution. We adopt a simple scheme which has the advantage of being analytically tractable [16]. Moreover, for a gas cooled below the recoil limit, the assumptions of the model can be justified in certain limits.

It is assumed that the width of the initial atomic velocity distribution is less than the recoil velocity $\hbar k/m$, i.e., $ku < \omega_k$. As a consequence, we can take the initial velocity distribution to be a δ function centered at $v=0$. In Fig. 3(a), the only states that are occupied initially are those in the $\{n,p=0\}$ manifold. Transitions occur to different manifolds that are initially unpopulated.

The next simplification results from the model we choose to describe relaxation and incoherent pumping of the atoms. It is assumed that, in the bare atom picture, level 1 decays at rate Γ_1, level 2 at rate Γ_2, and repopulation of level 1 by spontaneous emission from level 2 is

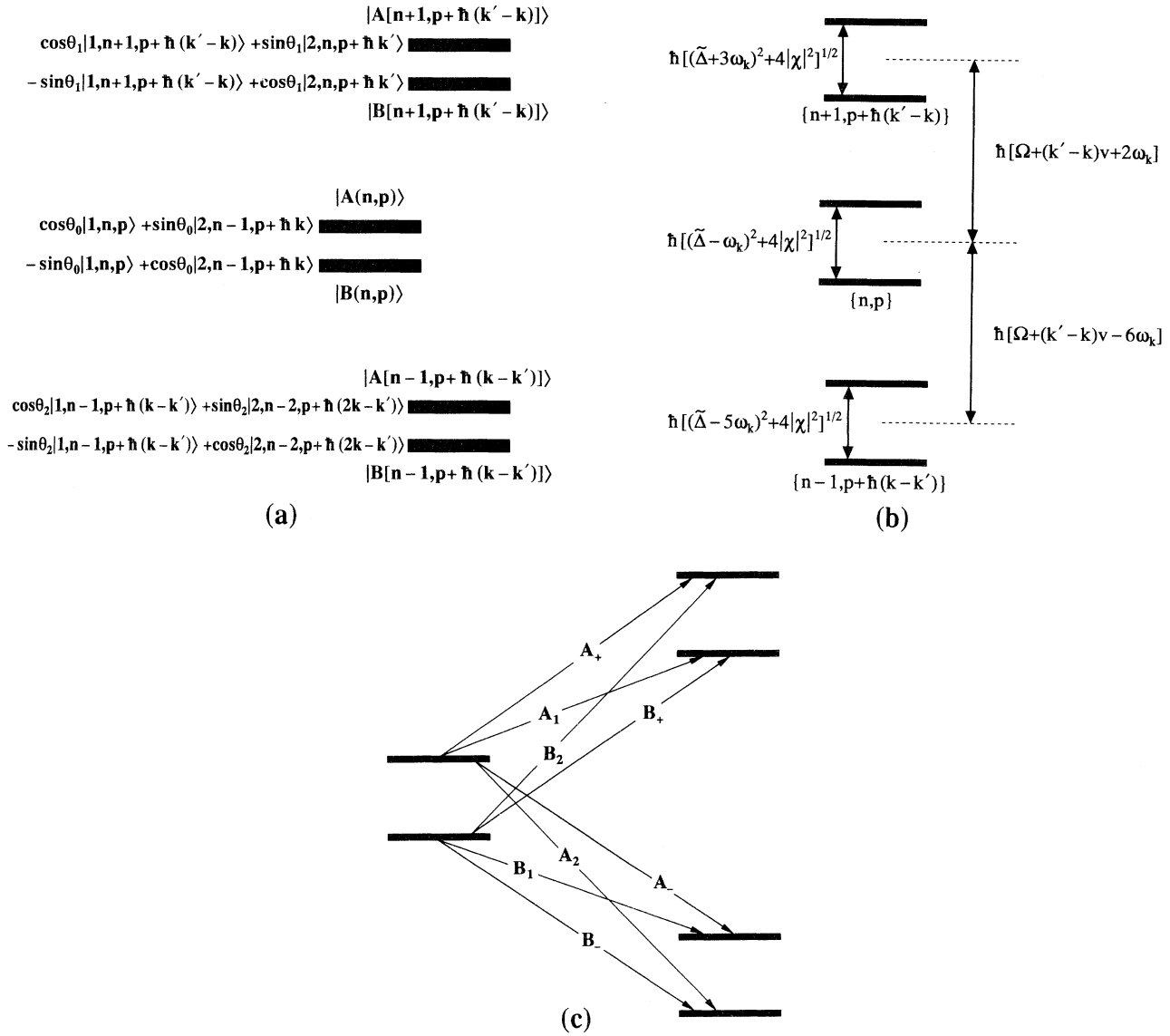

FIG. 3. (a) Dressed-state manifolds $\{n,p\}$, $\{n+1,p+\hbar(k'-k)\}$, and $\{n-1,p-\hbar(k'-k)\}$, along with the appropriate eigenstates. To zeroth order in ω_k/ω_{AB}, all the θ's are the same. (b) Energy level diagram. (c) Probe absorption and emission lines. Arrows A_1, B_2, A_+, and B_+ represent absorption and B_1, A_2, A_-, and B_- represent gain. These absorption and gain components are represented by the corresponding resonances shown in Fig. 2.

neglected. Level 1 is pumped incoherently at rate Λ. The decay rates and incoherent pumping rates for the dressed states are given by [17]

$$\Gamma_A=\Gamma_1\cos^2(\theta)+\Gamma_2\sin^2(\theta)\ ,$$
$$\Gamma_B=\Gamma_1\sin^2(\theta)+\Gamma_2\cos^2(\theta)\ , \tag{18}$$

and

$$\Lambda_A=\Lambda\cos^2(\theta)\ ,$$
$$\Lambda_B=\Lambda\sin^2(\theta)\ , \tag{19}$$

respectively. Since repopulation of level 1 is neglected, there is no cascade between the manifolds of the dressed states. In the secular approximation, where the coherence ρ_{AB} is neglected, one simply has to calculate the absorption of the probe field between two levels that decay incoherently out of the subsystem of levels under consideration.

There are eight transitions i ($i=A_1,B_1,A_2,B_2,A_+,B_+$) shown in Fig. 3(c) from the initial states $\mu=A(n,p=0)$ or $B(n,p=0)$ to the final states ν ($\nu=A[n+1,p=\hbar(k'-k)]$ or $B[n+1,p=\hbar(k'-k)]$ for absorption and $\nu=A[n-1,p=\hbar(k-k')]$ or $B[n-1,p=\hbar(k-k')]$ for emission). For a given transition i, centered at $\delta_i(\delta_i=\tilde{\delta}_i|_{v=0})$, the absorption coefficient is equal to [18]

$$\alpha_i=\pm 4\pi k\hbar^{-1}(\Lambda_\mu/\Gamma_\mu)|\langle\mu|d|\nu\rangle|^2\Gamma_i/[\Gamma_i^2+(\delta-\delta_i)^2]\ , \tag{20a}$$

where

$$\Gamma_i=\tfrac{1}{2}(\Gamma_\mu+\Gamma_\nu) \tag{20b}$$

is the homogeneous HWHM of the $\mu\rightarrow\nu$ transition and d is the dipole moment operator. The positive sign is chosen for absorption and negative for emission. Each SRC component is characterized by a Lorentzian line shape.

One can introduce a dimensionless line-shape function $F(\delta)$ defined by

$$\alpha=\alpha_0 F(\delta)\ , \tag{21a}$$

where

$$\alpha_0=4\pi k\hbar^{-1}\Lambda|\langle 2|d|1\rangle|^2/\Gamma_2^2\ . \tag{21b}$$

Near line center, a spectral component takes the limiting form

$$F(\delta)\approx\pm F_i L((\delta-\delta_i)/\Gamma_i)\ , \tag{22a}$$

where the function

$$L(x)=(1+x^2)^{-1} \tag{22b}$$

determines the shape of the spectral component, and the factor

$$F_i=(\Lambda_\mu/\Lambda)(\Gamma_2^2/\Gamma_\mu\Gamma_i)|M(i)|^2 \tag{22c}$$

with

$$|M(i)|^2=|\langle\mu|d|\nu\rangle/\langle 2|d|1\rangle|^2 \tag{22d}$$

determines its relative amplitude.

In calculating the matrix element $\langle\mu|d|\nu\rangle$ needed in Eq. (22d), using Eqs. (9), one finds that only those transitions between bare states having the same number of pump photons contribute. For example, the dipole matrix element which determines the amplitude F_{A_1} is given by

$$\langle A(n,p=0)|d|B(n+1,p=\hbar(k'-k))\rangle = \cos^2(\theta)\langle 1|d|2\rangle\ . \tag{23}$$

This matrix element, as well as the others needed in Eq. (22c), can be read directly from Fig. 3(a). The amplitudes and widths of the SRC whose resonance positions are defined in Eqs. (10)–(17) can be calculated using Eqs. (20b) and (22c) and Fig. 3(a). One obtains SRC amplitudes

$$F_{A_1}=[2/(1+\eta)]\cos^6(\theta)/[\sin^2(\theta)+\eta\cos^2(\theta)]\ , \tag{24a}$$

$$F_{B_1}=[2/(1+\eta)]\sin^2(\theta)\cos^4(\theta)/[\cos^2(\theta)+\eta\sin^2(\theta)]\ , \tag{24b}$$

$$F_{A_2}=[2/(1+\eta)]\cos^2(\theta)\sin^4(\theta)/[\sin^2(\theta)+\eta\cos^2(\theta)]\ , \tag{24c}$$

$$F_{B_2}=[2/(1+\eta)]\sin^6(\theta)/[\cos^2(\theta)+\eta\sin^2(\theta)]\ , \tag{24d}$$

$$F_{A_+}=F_{A_-}=\cos^4(\theta)\sin^2(\theta)/[\sin^2(\theta)+\eta\cos^2(\theta)]^2\ , \tag{24e}$$

$$F_{B_+}=F_{B_-}=\sin^4(\theta)\cos^2(\theta)/[\cos^2(\theta)+\eta\sin^2(\theta)]^2\ , \tag{24f}$$

where

$$\eta=\Gamma_1/\Gamma_2\ , \tag{24g}$$

and HWHMs

$$\Gamma_{A_1}=\Gamma_{A_2}=\Gamma_{B_1}=\Gamma_{B_2}=(\Gamma_1+\Gamma_2)/2\equiv\Gamma\ , \tag{25a}$$

$$\Gamma_{A_\pm}=\Gamma_A;\quad \Gamma_{B_\pm}=\Gamma_B\ . \tag{25b}$$

Note that in the limit

$$\eta\ll\tan^2(\theta)\ , \tag{26}$$

the results are independent of Γ_1.

IV. EXACT MODEL SOLUTION IN THE BARE STATE PICTURE

It is often useful to have theoretical expressions for the line shape that are not limited by the secular approximation. In this section a rigorous calculation of the probe absorption spectrum is given. Two-level atoms in an atomic vapor interact with an electric field of the form

$$E(x,t)=\tfrac{1}{2}[E\exp(-i\Omega t+ikx)+E'\exp(-i\Omega' t+ik'x)]+\text{c.c.}\ . \tag{27}$$

The pump and probe fields have amplitudes, frequencies, and wave vectors E, Ω, $\mathbf{k}=k\hat{\mathbf{x}}$ and E', Ω', $\mathbf{k}'=k'\hat{\mathbf{x}}$, respectively. Elements of the Wigner density matrix defined by

$$\rho(x,v)=(M/2\pi\hbar)V^{-1/3}\int dq\,\rho(p+\hbar q/2,p-\hbar q/2)\times\exp(iqx)\ , \tag{28}$$

where V is the gas volume and $\rho(p,p')$ is the density matrix in the momentum representation, evolve as

$$\dot{\rho}_{11}(x,v)+\Gamma_1\rho_{11}(x,v)=-i[\chi^* e^{i\Delta t-ikx}\rho_{21}(x,v+\xi)+\chi'^* e^{i\Delta' t-ik'x}\rho_{21}(x,v+\xi')-\text{c.c.}]+\Lambda f(v)\ , \tag{29a}$$

$$\dot{\rho}_{22}(x,v)+\Gamma_2\rho_{22}(x,v)=i[\chi^* e^{i\Delta t-ikx}\rho_{21}(x,v-\xi)+\chi'^* e^{i\Delta' t-ik'x}\rho_{21}(x,v+\xi')-\text{c.c.}]\ , \tag{29b}$$

$$\dot{\rho}_{21}(x,v)+\Gamma\rho_{21}(x,v)=-i\{\chi e^{-i\Delta t+ikx}[\rho_{11}(x,v-\xi)-\rho_{22}(x,v+\xi)]+\chi' e^{-i\Delta' t+ik'x}[\rho_{11}(x,v-\xi')-\rho_{22}(x,v+\xi')]\}\ , \tag{29c}$$

where $\dot{\rho}_{ik}=(\partial/\partial t+v\partial/\partial x)\rho_{ik}$,

$$\Gamma=\tfrac{1}{2}(\Gamma_1+\Gamma_2) \tag{30}$$

is the homogeneous HWHM,

$$\chi=-dE/2\hbar;\quad \chi'=-dE'/2\hbar \tag{31}$$

are Rabi frequencies,

$$\xi=\hbar k/2m;\quad \xi'=\hbar k'/2m \tag{32}$$

are recoil velocities, and $f(v)$ is the atomic distribution function in the absence of the field. An "in term," representing spontaneous emission from level 2 to 1, has not been included in Eq. (29a), consistent with the relaxation model adopted in Sec. III. In what follows, it is assumed that the pump and probe field counterpropagate relative to each other, $k'=-k$.

One can seek a steady-state solution to Eqs. (29) of the form

$$\rho_{ij}=\Lambda(R_{ij}+r_{ij})\ , \tag{33}$$

where R_{ij} and r_{ij} are zeroth and first order in χ', respectively. By defining

$$R_{ii}(x,v)\equiv R_i(v)\ , \tag{34a}$$

$$R_{12}(x,v)\equiv i\chi^*\exp(i\Delta t-ikx)R(v)\ , \tag{34b}$$

$$r_{jj}(x,v)\equiv\exp[-i\delta t+i(k'-k)x]r_j(v)+\text{c.c.}\ , \tag{34c}$$

$$r_{21}(x,v)\equiv r(v)\exp[-i\Delta' t+ik'x]+\tilde{r}^*(v)\exp[-i(2\Delta-\Delta')t+i(2k-k')x]\ , \tag{34d}$$

one can use Eqs. (29) to obtain the coupled equations

$$\Gamma_1 R_1(v)=-2|\chi|^2\text{Re}[R(v+\xi)]+f(v)\ , \tag{35a}$$

$$\Gamma_2 R_2(v)=2|\chi|^2\text{Re}[R(v-\xi)]\ , \tag{35b}$$

$$\mu^*(v)R(v)=R_1(v-\xi)-R_2(v+\xi)\ ; \tag{35c}$$

$$\mu'(v)r(v)=-i\chi[r_1(v-\xi)-r_2(v+\xi)]-i\chi'[R_1(v-\xi')-R_2(v+\xi')]\ , \tag{36a}$$

$$\tilde{\mu}(v)\tilde{r}(v)=i\chi^*[r_1(v-\xi)-r_2(v+\xi)]\ , \tag{36b}$$

$$\mu_1(v)r_1(v)=-i\chi^* r(v+\xi)+i\chi\tilde{r}(v+\xi)-\chi'\chi^* R(v+\xi')\ , \tag{36c}$$

$$\mu_2(v)r_2(v)=i\chi^* r(v-\xi)-i\chi\tilde{r}(v-\xi)+\chi'\chi^* R(v-\xi')\ , \tag{36d}$$

where

$$\mu(v)=\Gamma-i(\Delta-kv)\ , \tag{37a}$$

$$\mu'(v)=\Gamma-i(\Delta'-k'v)\ , \tag{37b}$$

$$\tilde{\mu}(v)=\Gamma+i[\Delta-\delta-(2k-k')v]\ , \tag{37c}$$

$$\mu_j(v)=\Gamma_j-i[\delta-(k'-k)v]\ . \tag{37d}$$

If one chooses as variables $\{R_1(v),R(v+\xi),R_2(v+2\xi)\}$ and $\{r(v),\tilde{r}(v),r_1(v-\xi),r_2(v+\xi)\}$ in Eqs. (35) and (36), respectively, the equations become algebraic in nature and can be solved easily.

The positive frequency part of the atomic polarization P which varies as $\exp[i(k'x-\Omega' t)]$ is given by

$$P=\Lambda\langle 1|d|2\rangle\langle r(v)\rangle\ , \tag{38}$$

where $\langle\ \rangle$ indicates an average over velocities. The probe absorption coefficient $\alpha=4\pi k\,\text{Im}(2P/E')$ is obtained from Eqs. (35), (36), and (38) as

$$\alpha=\alpha_0 F(\delta)\ , \tag{39}$$

where α_0 is defined by Eq. (21b),

$$F(\delta)=\Gamma_2^2\text{Re}\langle(\mu'(v)\{1+|\chi|^2[1/\mu'(v)+1/\tilde{\mu}(v)][1/\mu_1(v-\xi)+1/\mu_2(v+\xi)]\})^{-1}\times(\{1+[|\chi|^2/\tilde{\mu}(v)][1/\mu_1(v-\xi)+1/\mu_2(v+\xi)]\}[R_1(v-\xi')-R_2(v+\xi')]-|\chi|^2[R(v+\xi'-\xi)/\mu_1(v-\xi)+R(v-\xi'+\xi)/\mu_2(v+\xi)])\rangle\ , \tag{40}$$

$$R_1(v)=\Gamma_1^{-1}\{1-I[\Gamma_2/(\Gamma_1+\Gamma_2)]\Gamma^2[|\mu(v+\xi)|^2+I\Gamma^2]^{-1}\}f(v)\ , \tag{41a}$$

$$R_2(v)=[I/(\Gamma_1+\Gamma_2)]\Gamma^2[|\mu(v-\xi)|^2+I\Gamma^2]^{-1}f(v-2\xi)\ , \tag{41b}$$

$$R(v)=\mu(v)[\Gamma_1(|\mu(v)|^2+I\Gamma^2)]^{-1}f(v-\xi)\ ; \tag{41c}$$

and

$$I=4|\chi|^2/\Gamma_1\Gamma_2 \tag{42}$$

is a saturation parameter.

For atoms cooled below the recoil limit one can set

$$f(v)=\delta(v)\ , \tag{43}$$

implying that

$$R_1(v)=R_1\delta(v),\quad R_1=[R_1(v)/f(v)]_{v=0}\ , \tag{44a}$$

$$R_2(v)=R_2\delta(v-2\xi),\quad R_2=[R_2(v)/f(v-2\xi)]_{v=2\xi}\ , \tag{44b}$$

$$R(v)=R\delta(v-\xi),\quad R=[R(v)/f(v-\xi)]_{v=\xi}\ . \tag{44c}$$

By combining Eqs. (40), (41), and (42) one obtains finally

$$\alpha=\alpha_0F(\delta)\ , \tag{45}$$

where

$$\begin{aligned}F(\delta)=\Gamma_2^2\mathrm{Re}[&(\mu'(\xi')\{1+|\chi|^2[1/\mu'(\xi')+1/\tilde{\mu}(\xi')][1/\mu_1(\xi'-\xi)+1/\mu_2(\xi'+\xi)]\})^{-1}\\ &\times(\{1+[|\chi|^2/\tilde{\mu}(\xi')][1/\mu_1(\xi'-\xi)+1/\mu_2(\xi'+\xi)]\}R_1-|\chi|^2R/\mu_2(\xi'+\xi))\\ &-(\mu'(2\xi-\xi')\{1+|\chi|^2[1/\mu'(2\xi-\xi')+1/\tilde{\mu}(2\xi-\xi')][1/\mu_1(\xi-\xi')+1/\mu_2(3\xi-\xi')]\})^{-1}\\ &\times(\{1+[|\chi|^2/\tilde{\mu}(2\xi-\xi')][1/\mu_1(\xi-\xi')+1/\mu_2(3\xi-\xi')]\}R_2+|\chi|^2R/\mu_1(\xi-\xi'))]\ .\end{aligned} \tag{46}$$

After some algebraic manipulations, the exact solution (46) reduces to the SRC line shapes [(22a) or (A15)–(A32)] provided the secular limit

$$\omega_{AB}\gg\Gamma \tag{47}$$

holds; however, the individual SRC resonances may not be resolved unless $\omega_k>\Gamma$. Note that condition (47) puts no restriction on the ratio ω_k/Γ.

V. DISCUSSION

Expression have been derived which determine the probe absorption spectrum associated with a given atomic transition when that transition is simultaneously driven by a pump field having arbitrary intensity. In the limit that the recoil frequency is larger than the various relaxation rates, the spectrum consists of eight resolved components, four corresponding to absorption and four to emission. The positions, widths, and relative amplitudes of these components can be predicted using a dressed-atom approach that includes the center-of-mass energy in the definition of the dressed states. Despite the fact that the dressed-atom picture completely characterizes the spectrum, additional insight into the origin of the various resonances can be obtained by considering the lowest-order nonvanishing contributions to the resonances using a bare atom picture (see, also, Ref. [16]). It is convenient to analyze the resonances in terms of the pairs (A_1,B_1), (A_2,B_2), $A_\pm,B_\pm$ [see Fig. 3(c)]. It is assumed that $\theta\simeq|\chi/\Delta|^2$ is a small quantity and that $|\Delta|\gg\Gamma$.

(A_1,B_1). The amplitude corresponding to the lowest order (in pump field strength) contribution to the A_1 resonance is shown schematically in Fig. 4(a). The absorption probability associated with this amplitude is proportional to the product of the steady-state population of level 1 (Λ/Γ_1) multiplied by a Lorentzian having HWHM $\Gamma=(\Gamma_1+\Gamma_2)/2$. The position of the resonance, obtained from the conservation of energy condition

$$\hbar\omega-\hbar\Omega'+\epsilon_{\hbar k'}=0 \tag{48a}$$

is

$$\delta_{A_1}=-\Delta+\omega_k\ , \tag{48b}$$

which coincides with Eq. (10) in the weak pump field limit.

The diagram corresponding to the lowest-order contribution to the B_1 resonance is shown schematically in Fig. 5(a). This contribution is again proportional to a Lorentzian factor having HWHM Γ. However, in this case the emission probability is proportional to the "incoherent" population of level 2, represented schematically in the diagram by the thick arrow. If level 2 were pumped incoherently at rate Λ_2, this population would be equal to Λ_2/Γ_2 and the emission resonance would be centered at $\delta=-\Delta-\omega_k$. In our model, however, the population of level 2 results from the action of the pump field.

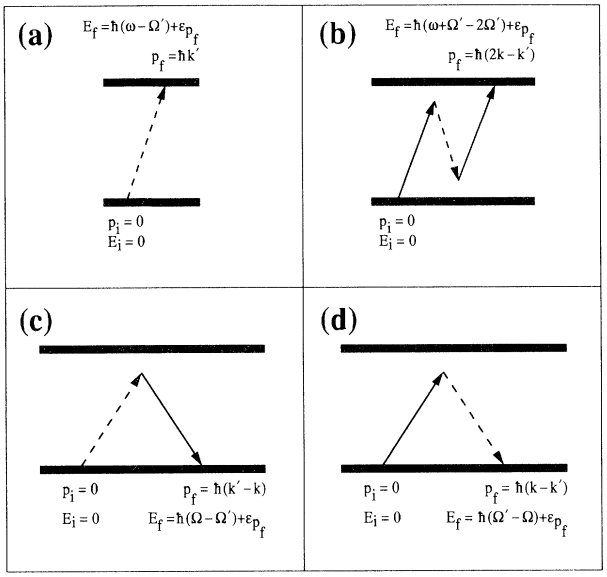

FIG. 4. Schematic representation of the multiphoton processes in the weak pump field limit (bare atom picture). Solid and dashed arrows correspond to the interaction with pump and probe field, respectively. Each diagram corresponds to a transition amplitude starting from level 1. Diagrams (a), (b), (c), and (d) contribute to SRCs A_1, A_2, A_+, and A_-, respectively. Positions of these SRCs are determined by the conservation energy law, $E_i=E_f$. Initial and final state values for the atomic momenta and energies are given.

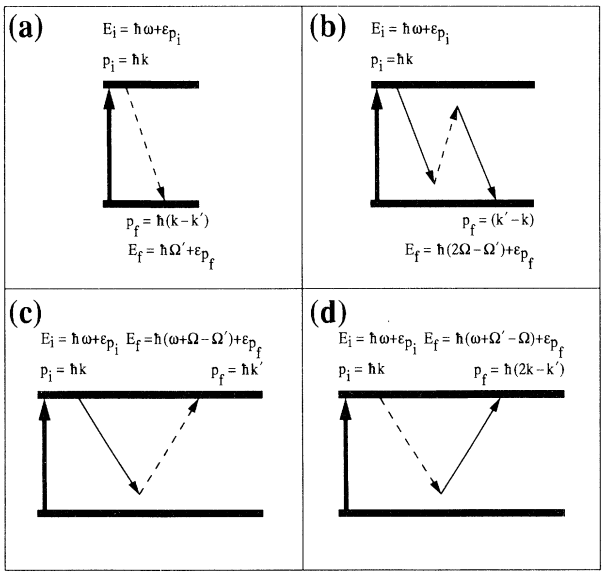

FIG. 5. Diagrams, similar to those shown in Fig. 4, for transitions originating on level 2. The broad arrow represents a process in which the pump field provides an "incoherent" contribution to the population of level 2, in which the upper state atoms acquire a momentum of $\hbar k$. Diagrams (a), (b), (c), and (d) contribute to SRCs B_1, B_2B_+, and B_-, respectively.

The "incoherent" population of level 2 (which is nothing more than the steady-state population of the dressed state $|B\rangle$ in the weak-field limit) is proportional to $(\Lambda_1/\Gamma_1)(\Gamma_1/\Gamma_2)\theta^2=(\Lambda/\Gamma_2)\theta^2$ if $\Gamma_1\neq 0$ [19]. Since the population of level 2 is created with momentum $p=\hbar k$, conservation of energy requires that

$$\hbar\omega+\epsilon_{\hbar k}=\hbar\Omega'+\epsilon_{\hbar(k-k')} \tag{49a}$$

or

$$\delta_{B_1}=-\Delta+\hbar k'(2k-k')/2m=-\Delta-3\omega_k \tag{49b}$$

for $k'=-k$, in agreement with Eq. (11). The ratio of the B_1 to A_1 amplitudes is proportional to $(\Gamma_1/\Gamma_2)\theta^2$, in agreement with Eqs. (24a) and (24b) in the limit that $\theta\sim 0$. (In the limit that $\Gamma_2\theta^2>\Gamma_1$, the above result is modified since saturation of the system must be accounted for even in this weak-field limit. In that limit, we must replace Γ_1 by $\Gamma_2\theta^2$, such that the ratio of the B_1 to A_1 amplitudes becomes proportional to θ^4. In this manner, the results become independent of Γ_1, simulating the results that would have been obtained had we considered a "closed" system in which the sum of ground-state plus excited-state populations was conserved [20].)

The resonances are separated in frequency by $4\omega_k$; consequently, they can be resolved only if $4\omega_k>2\Gamma$. This can be achieved if one uses forbidden transitions such as those in Mg at $\lambda=0.447\mu$ and Ca at $\lambda=0.653\mu$. The portion of the pump-probe spectrum containing SRCs A_1 and B_1 is shown in Fig. 6.

(A_2,B_2). The analysis of these resonances is similar to that for the (A_1,B_1) resonances. The corresponding diagrams for the A_2 and B_2 amplitudes are shown in Figs. 4(b) and 5(b), respectively. The A_2 resonance has HWHM Γ, amplitude proportional to $(\Lambda/\Gamma_1)\theta^4$, and is

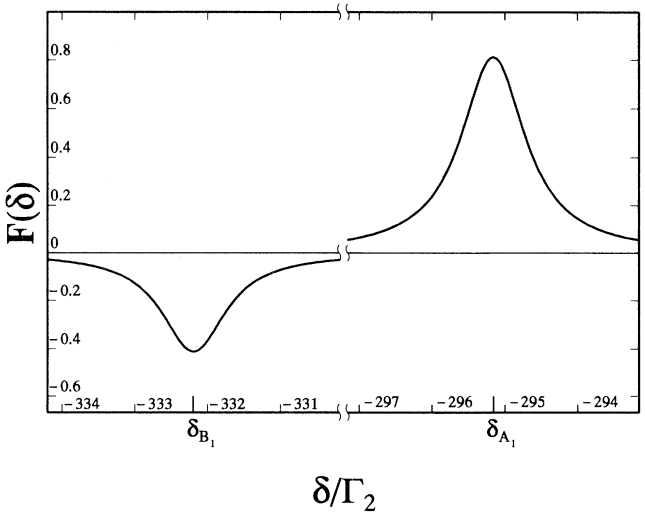

FIG. 6. A_1 and B_1 SRC for $\Delta/\Gamma_2=50$, $\chi/\Gamma_2=150$, $\omega_k/\Gamma_2=5$, and $\Gamma_1/\Gamma_2=0.05$. Γ_2 is arbitrarily set equal to unity in this and subsequent graphs. These components collapse to the absorption component shown in Fig. 1 in the weak-pump-field limit in the absence of recoil.

centered at $\delta=\Delta-\hbar(2k-k')^2/2m=\Delta-9\omega_k$ for $k'=-k$. The B_2 resonance has HWHM Γ, amplitude proportional to $(\Lambda\theta^2/\Gamma_2)\theta^4$, and is centered at $\delta=\Delta-\hbar k'(2k-k')/2m=\Delta+3\omega_k$ for $k'=-k$. These results are in agreement with Eqs. (12), (13), (24c), (24d), and (25a) in the limit $\theta\sim 0$. The resonances are separated in frequency by $12\omega_k$ and can be resolved only if $12\omega_k>2\Gamma$. The portion of the pump-probe spectrum containing SRCs A_2 and B_2 is shown in Fig. 7.

$A_\pm$. The diagrams corresponding to these resonances are shown in Figs. 4(c) and 4(d), respectively. The A_+ absorption peak has HWHM Γ_1, amplitude proportional to $(\Lambda/\Gamma_1)\theta^2$, and is centered at $\delta=\hbar(k-k')^2/2m=4\omega_k$ for $k'=-k$. The A_- emission peak has HWHM Γ_1, amplitude proportional to $(\Lambda/\Gamma_1)\theta^2$, and is centered at $\delta=-\hbar[k-k']^2/2m=-4\omega_k$ for $k'=-k$. These results are in agreement with Eqs. (14), (15), (24e), and (25b) in the limit $\theta\sim 0$. The resonances are separated in frequency by $8\omega_k$ and are resolved if $8\omega_k>\Gamma_1$.

The $A_\pm$ resonances correspond to the RIR which have been discussed previously [8–12]. In those discussions, the residual Doppler width, $(k-k')u=2ku$, is assumed to be larger than the recoil frequency. As such, *the final states involved in there transitions shown in Fig. 3(b) are also populated.* The absorption and emission profiles then depend on the integrals of Eqs. (20a) (with $\delta+2kv$ replacing δ in those equations) over velocity with a weighting function given by $[f(v)-f(v\mp 2\hbar k/m)]$, which represents the difference between initial and final state populations. The resulting sum of absorption and emission components is proportional to $df(v)/dv$ evaluated at $v=\delta/2k$.

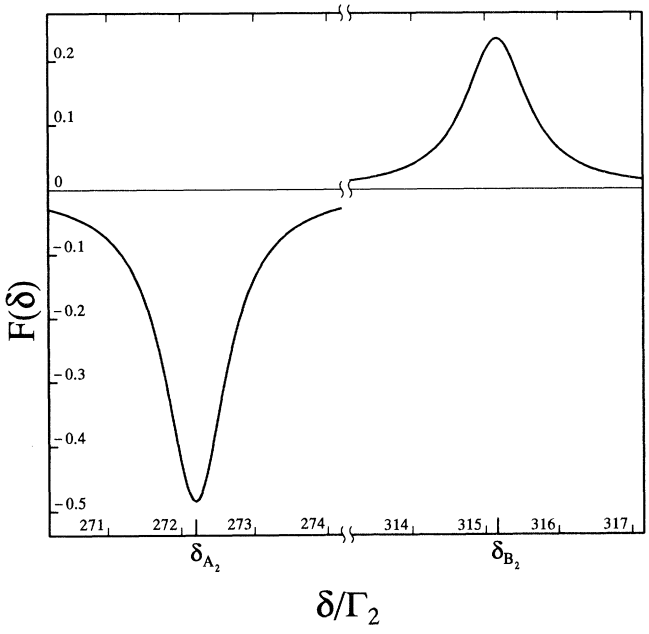

FIG. 7. A_2 and B_2 SRC for $\Delta/\Gamma_2=50$, $\chi/\Gamma_2=150$, $\omega_k/\Gamma_2=5$, and $\Gamma_1/\Gamma_2=0.05$. These components collapse to the emission component shown in Fig. 1 in the weak-pump-field limit in the absence of recoil.

$B_\pm$. The diagrams corresponding to these resonances are shown in Figs. 5(c) and 5(d), respectively. The B_+ absorption peak has HWHM Γ_2, amplitude proportional to $(\Lambda\theta^2/\Gamma_2)\theta^2$, and is centered at $\delta=(\hbar/2m)\{k^2-[k+(k'-k)]^2\}=0$ for $k'=k$. The B_- emission peak has HWHM Γ_2, amplitude proportional to $(\Lambda\theta^2/\Gamma_2)\theta^2$, and is centered at $\delta=(\hbar/2m)\{k^2-[k+(k-k')]^2\}=-8\omega_k$ for $k'=-k$. These results are in agreement with Eqs. (16), (17), (24f), and (25b) in the limit $\theta\sim 0$. The resonances are separated in frequency by $8\omega_k$ and are resolved if $8\omega_k>\Gamma_2$. These resonances are smaller than the $A_\pm$ resonances by a factor $(\Gamma_1\theta^2/\Gamma_2)$ [or θ^4, if $\Gamma_2\theta^2>\Gamma_1$]. The two components of each of the $A_\pm$ and $B_\pm$ resonance doublets cancel one another in the limit $\omega_k\sim 0$. The portion of the pump-probe spectrum containing SRCs $A_\pm$ and $B_\pm$ is shown in Fig. 8.

The eight component spectrum can be seen only if $\omega_k>2\Gamma$, a limit that can be achieved only for forbidden transitions or for transitions between a high lying Rydberg state and a low lying electronic state [21]. In the limit $2\Gamma>\omega_k$ typical of allowed transitions, the (A_1,B_1) doublet collapses to a single absorption line, the (A_2,B_2) doublet collapses to a single emission component, and the $B_\pm$ resonances centered near $\delta=0$ collapse into a dispersionlike structure whose amplitude is negligible compared with the $A_\pm$ resonances provided that the ratio Γ_A/Γ_B of dressed-state decay rates is much less than unity. The $A_\pm$ resonances are resolved if

$$8\omega_k>\Gamma_A=[\Gamma_1\cos^2(\theta)+\Gamma_2\sin^2(\theta)]\ . \tag{50}$$

In the limit that $(\Gamma_1/\Gamma_2)\ll\theta^2\ll 1$, condition (50) is satisfied if $8\omega_k>\Gamma_2\theta^2$. In somewhat stronger fields such that $\Gamma_2\sin^2(\theta)>8\omega_k$, the $A_\pm$ resonances collapse into a dispersionlike structure.

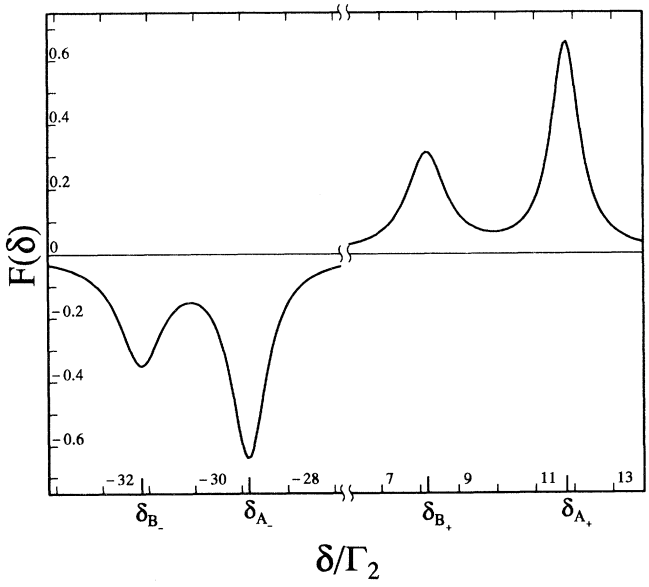

FIG. 8. $A_\pm$ and $B_\pm$ SRC for $\Delta/\Gamma_2=50$, $\chi/\Gamma_2=150$, $\omega_k/\Gamma_2=5$, and $\Gamma_1/\Gamma_2=0.05$. In the weak-pump-field limit and the secular approximation, these components cancel one another in the absence of recoil.

Since the SRCs displayed in Figs. 6–8 were obtained in the secular limit, $(\Gamma_2/\omega_{AB})\sim 0.0033$, they can be calculated using either the dressed state expressions or the exact line shape. For larger values of Γ_2/ω_{AB}, the exact line shape expression must be used. This feature is illustrated in Fig. 9 for the $A_\pm$ resonances. The non-secular contribution becomes important only when the recoil splitting is no longer totally resolved; the ratio of the secular to nonsecular terms is of order $8\omega_k\omega_{AB}/(\Gamma_A\Gamma)$.

It is interesting also to consider the spectrum when the pump field is resonant, $\Delta=0$. It is well known [1,3] that, in the absence of recoil and in the secular approximation, the probe field absorption coefficient vanishes in the whole spectral region. The vanishing of the probe spectrum results from the mutual cancellation of the emission and absorption SRCs which no longer occurs when the recoil splitting of the components is taken into account. The $\Delta=0$ emission SRCs A_- and B_- (absorption SRCs A_+ and B_+) are centered at the same point $\delta_{A_-,B_-}=-6\omega_k(\delta_{A_+,B_+}=2\omega_k)$ and the four central components located near $\delta\sim 0$ degenerate into a doublet whose amplitude is twice that of the components centered near $\tilde{\delta}\approx\pm\omega_{AB}$. A pump-probe line shape for $\Delta=0$ is plotted in Fig. 10.

All effects related to atomic recoil resulting from spontaneous emission from level 2 to 1 have been neglected in this work. Spontaneous emission processes of this type would broaden the subrecoil velocity distribution of the atoms. For resolved recoil components, $(\Gamma_i/\omega_k)\ll 1$, where Γ_i is the width of one of the components shown in Figs. 6–8, spontaneous emission leads to a broad background having a width of order $k(\hbar k/m)=2\omega_k$. The amplitude of the background term is reduced from that of the SRCs by at least a factor $\Gamma_i/\omega_k\ll 1$ and can be neglected. For components having $\Gamma_i/\omega_k\gtrsim 1$, spontaneous emission leads to perturbative corrections to the density matrix; however, the *integrated* contribution of these corrections may not be negligible and must be included in the theory.

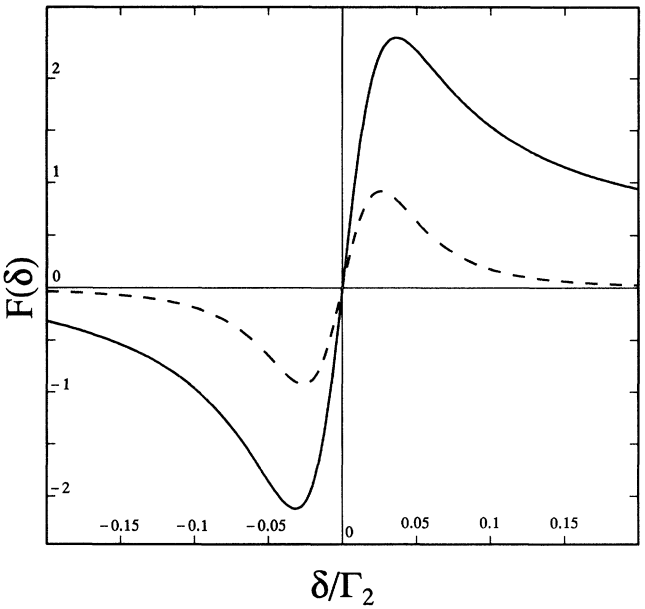

FIG. 9. $A_\pm$ resonances for $\Delta/\Gamma_2=5$, $\chi/\Gamma_2=1$, $\omega_k/\Gamma_2=5.0\times 10^{-4}$, and $\Gamma_1/\Gamma_2=0.01$. The solid curve is a graph of the exact expression for the line shape, while the dashed curve is obtained from the dressed-state theory in the secular approximation. The parameter $8\omega_k\omega_{AB}/(\Gamma_A\Gamma)$, which is a measure of the relative amplitude of the secular to nonsecular contributions, is equal to unity.

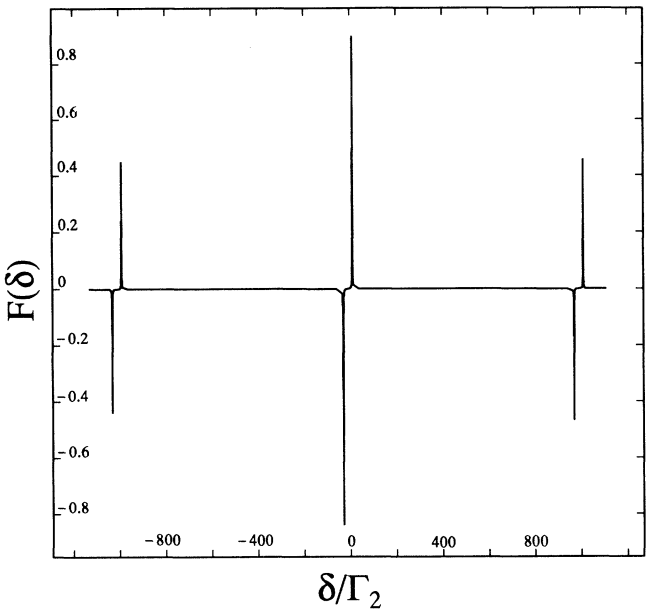

FIG. 10. Probe absorption line shape for $\Delta/\Gamma_2=0$, $\chi/\Gamma_2=500$, $\omega_k/\Gamma_2=5$, and $\Gamma_1/\Gamma_2=0.05$. The eight components collapse into six each having HWHM equal to Γ.

In our model, incoherent pumping at rate Λ always supplies new atoms to the interaction volume. In experimental situations of interest, one often encounters closed systems in which overall population of the atomic states is conserved, but there is no incoherent pumping. In this limit, the role of spontaneous emission must be examined in more detail, since spontaneous emission can effectively prevent atoms from interacting with the external fields by moving them out of resonance with the fields. In general, one must treat the atom-field interaction in the transient rather than steady-state domain to obtain the appropriate line shapes.

Finally, we note that the SRC emission lines can be used for probe field amplification, including frequency up- or down-conversion. For a beam of cold atoms having velocity $\mathbf{v}_0=v_0\hat{\mathbf{x}}$, probe field amplification occurs at the center of a gain component when

$$\Omega'-\Omega=\tilde{\delta}_i-2kv_0\ . \tag{51}$$

For $v_0<0$ and $k|v_0|\gg\tilde{\delta}_i$, one achieves frequency upconversion by an amount $2k|v_0|$. Effects of this type are now

discussed in the literature for the both nonrelativistic [13] and relativistic [22] atomic beams.

ACKNOWLEDGMENTS

This work was supported by the U.S. Army Research Office and by the National Science Foundation under Grant No. PHY 9396245 and through the Center for Ultrafast Optical Science under Grant No. STC PHY 8920108. J.G. was supported by the E.U. Condon Postdoctoral Fellowship Program at JILA.

APPENDIX

In this appendix, we generalize the dressed-state calculations to allow for an arbitrary ratio of ω_k to ω_{AB}. Equations are derived for an initial state manifold having $p=0$, but they are easily generalized to nonzero p by the substitutions $\delta\rightarrow\tilde{\delta}=\delta+(k-k')v$ and $\Delta\rightarrow\tilde{\Delta}=\Delta-kv$. We consider only the case $(k-k')=2k$, but the results can be generalized to allow for arbitrary $(k-k')$.

The energy levels of the three manifolds of levels shown in Fig. 3 can be obtained from Eq. (6) as [23]

$$E(n,p=0)=\hbar[-\Delta+\omega_k\pm\sqrt{(\Delta-\omega_k)^2+4|\chi|^2}]/2\ , \tag{A1}$$

$$E(n+1,p=-2\hbar k)=\hbar\Omega+\hbar[-\Delta+5\omega_k\pm\sqrt{(\Delta+3\omega_k)^2+4|\chi|^2}]/2\ , \tag{A2}$$

$$E(n+1,p=2\hbar k)=-\hbar\Omega+\hbar[-\Delta+13\omega_k\pm\sqrt{(\Delta-5\omega_k)^2+4|\chi|^2}]/2\ . \tag{A3}$$

The eigenvectors are still given by Eq. (9), but the value of θ differs for the three manifolds. Referring to the $\{n,p=0\}$, $\{n+1,p=-2\hbar k\}$ and $\{n-1,p=2\hbar k\}$ manifolds as manifolds 0, 1, and 2, respectively, one can use Eqs. (4), (6), and (9) to obtain

$$\cos^2(\theta_0)=[1+(\Delta-\omega_k)/\sqrt{(\Delta-\omega_k)^2+4|\chi|^2}]/2\ , \tag{A4}$$

$$\cos^2(\theta_1)=[1+(\Delta+3\omega_k)/\sqrt{(\Delta+3\omega_k)^2+4|\chi|^2}]/2\ , \tag{A5}$$

$$\cos^2(\theta_2)=[1+(\Delta-5\omega_k)/\sqrt{(\Delta-5\omega_k)^2+4|\chi|^2}]/2\ . \tag{A6}$$

The positions, widths and amplitudes of the various resonances can now be read directly from Fig. 3. The positions are given by

$$\delta_{A_1}=2\omega_k-[\sqrt{(\Delta+3\omega_k)^2+4|\chi|^2}+\sqrt{(\Delta-\omega_k)^2+4|\chi|^2}]/2\ , \tag{A7}$$

$$\delta_{B_1}=-6\omega_k-[\sqrt{(\Delta-\omega_k)^2+4|\chi|^2}+\sqrt{(\Delta-5\omega_k)^2+4|\chi|^2}]/2\ , \tag{A8}$$

$$\delta_{A_2}=-6\omega_k+[\sqrt{(\Delta-\omega_k)^2+4|\chi|^2}+\sqrt{(\Delta-5\omega_k)^2+4|\chi|^2}]/2\ , \tag{A9}$$

$$\delta_{B_2}=2\omega_k+[\sqrt{(\Delta+3\omega_k)^2+4|\chi|^2}+\sqrt{(\Delta-\omega_k)^2+4|\chi|^2}]/2\ , \tag{A10}$$

$$\delta_{A_+}=2\omega_k+[\sqrt{(\Delta+3\omega_k)^2+4|\chi|^2}-\sqrt{(\Delta-\omega_k)^2+4|\chi|^2}]/2\ , \tag{A11}$$

$$\delta_{A_-}=-6\omega_k+[\sqrt{(\Delta-\omega_k)^2+4|\chi|^2}-\sqrt{(\Delta-5\omega_k)^2+4|\chi|^2}]/2\ , \tag{A12}$$

$$\delta_{B_+}=2\omega_k-[\sqrt{(\Delta+3\omega_k)^2+4|\chi|^2}-\sqrt{(\Delta-\omega_k)^2+4|\chi|^2}]/2\ , \tag{A13}$$

$$\delta_{B_-}=-6\omega_k-[\sqrt{(\Delta-\omega_k)^2+4|\chi|^2}-\sqrt{(\Delta-5\omega_k)^2+4|\chi|^2}]/2\ . \tag{A14}$$

The SRC amplitudes are obtained from Eqs. (22c) and (22d), which can be evaluated once the Λ's, Γ's, and M's are given. The transition HWHMs are one-half the sum of the decay rates of the two levels involved in a given transition. For all the A transitions,

$$\Lambda_A=\Lambda\cos^2(\theta_0);\Gamma_A=\Gamma_1\cos^2(\theta)+\Gamma_2\sin^2(\theta)\ , \tag{A15}$$

and for all the B transitions,

$$\Lambda_B=\Lambda\sin^2(\theta_0);\Gamma_B=\Gamma_2\cos^2(\theta)+\Gamma_1\sin^2(\theta)\ . \tag{A16}$$

The HWHMs of the transitions are given by

$$\Gamma_{A_1}=\{\Gamma_1[\cos^2(\theta_0)+\sin^2(\theta_1)]+\Gamma_2[\sin^2(\theta_0)+\cos^2(\theta_1)]\}/2\ , \tag{A17}$$

$$\Gamma_{B_1}=\{\Gamma_1[\cos^2(\theta_2)+\sin^2(\theta_0)]+\Gamma_2[\sin^2(\theta_2)+\cos^2(\theta_0)]\}/2\ , \tag{A18}$$

$$\Gamma_{A_2}=\{\Gamma_1[\cos^2(\theta_0)+\sin^2(\theta_2)]+\Gamma_2[\sin^2(\theta_0)+\cos^2(\theta_2)]\}/2\ , \tag{A19}$$

$$\Gamma_{B_2}=\{\Gamma_1[\cos^2(\theta_1)+\sin^2(\theta_0)]+\Gamma_2[\sin^2(\theta_1)+\cos^2(\theta_0)]\}/2\ , \tag{A20}$$

$$\Gamma_{A_+}=\{\Gamma_1[\cos^2(\theta_0)+\cos^2(\theta_1)]+\Gamma_2[\sin^2(\theta_0)+\sin^2(\theta_1)]\}/2\ , \tag{A21}$$

$$\Gamma_{A_-}=\{\Gamma_1[\cos^2\theta_0+\cos^2(\theta_2)]+\Gamma_2[\sin^2\theta_0+\sin^2(\theta_2)]\}/2\ , \tag{A22}$$

$$\Gamma_{B_+}=\{\Gamma_2[\cos^2(\theta_0)+\cos^2(\theta_1)] +\Gamma_1[\sin^2(\theta_0)+\sin^2(\theta_1)]\}/2 , \quad \text{(A23)}$$

$$\Gamma_{B_-}=\{\Gamma_2[\cos^2(\theta_0)+\cos^2(\theta_2)] +\Gamma_1[\sin^2\theta_0+\sin^2(\theta_2)]\}/2 . \quad \text{(A24)}$$

Finally, the matrix elements needed in Eq. (22d) are now given by

$$|M(A_1)|^2=\cos^2(\theta_0)\cos^2(\theta_1) , \quad \text{(A25)}$$

$$|M(B_1)|^2=\cos^2(\theta_0)\cos^2(\theta_2) , \quad \text{(A26)}$$

$$|M(A_2)|^2=\sin^2(\theta_0)\sin^2(\theta_2) , \quad \text{(A27)}$$

$$|M(B_2)|^2=\sin^2(\theta_0)\sin^2(\theta_1) , \quad \text{(A28)}$$

$$|M(A_+)|^2=\cos^2(\theta_0)\sin^2(\theta_1) , \quad \text{(A29)}$$

$$|M(A_-)|^2=\sin^2(\theta_0)\cos^2(\theta_2) , \quad \text{(A30)}$$

$$|M(B_+)|^2=\sin^2(\theta_0)\cos^2(\theta_1) , \quad \text{(A31)}$$

$$|M(B_-)|^2=\cos^2(\theta_0)\sin^2(\theta_2) . \quad \text{(A32)}$$

For example, the amplitude of the A_1 SRC is $(\Lambda_A/\Lambda)[\Gamma^2/(\Gamma_{A_1}\Gamma_A)]|M(A_1)|^2$, while that of the B_2 SRC is $(\Lambda_B/\Lambda)[\Gamma^2/(\Gamma_{B_2}\Gamma_B)]|M(B_2)|^2$.

[1] B. R. Mollow, Phys. Rev. A **5**, 2217 (1972). See also, G. Khitrova, P. R. Berman, and M. Sargent III, J. Opt. Soc. Am. B **5**, 160 (1988), and references therein; M. T. Gruneisen, K. R. MacDonald, and R. W. Boyd, *ibid.* **5**, 122 (1988); G. Grynberg and C. Cohen-Tannoudji, Opt. Commun. **96**, 150 (1993).

[2] F. Y. Wu, S. Ezekiel, M. Ducloy, and B. R. Mollow, Phys. Rev. Lett. **38**, 1077 (1977).

[3] C. Cohen-Tannoudji and S. Reynaud, J. Phys. B **10**, 345 (1977); C. Cohen-Tannoudji, J. Dupont-Roc, and G. Grynberg, *Atom-Photon Interactions* (Wiley, New York, 1992), Chap. 6.

[4] A. P. Kol'chenko, S. G. Rautian, and R. I. Sokolovskii, Zh. Eksp. Teor. Fiz. **55**, 1864 (1968) [Sov. Phys. JETP **55**, 986 (1968)].

[5] See, for example, J. L. Hall, C. Bordé, and K. Uehara, Phys. Rev. Lett. **37**, 1339 (1976).

[6] See, for example, J. C. Bergquist, R. L. Barger, and D. J. Glaze, in *Laser Spectroscopy IV,* edited by H. Walther and K. W. Rothe (Springer-Verlag, Berlin, 1979), pp. 120–129; F. Riehle, Th. Kisters, A. Witte, J. Helmcke, and C. Bordé, Phys. Rev. Lett. **67**, 177 (1991); U. Steer, K. Sengstock, J. H. Muller, D. Bettermann, and W. Ertmer, Appl. Phys. B **54**, 341 (1992).

[7] D. S. Weiss, B. C. Young, and S. Chu, Phys. Rev. Lett. **70**, 2706 (1993).

[8] J. Guo, P. R. Berman, B. Dubetsky, and G. Grynberg, Phys. Rev. A **46**, 1426 (1992).

[9] J. Y. Courtois, G. Grynberg, B. Lounis, and P. Verkerk, Phys. Rev. Lett. **72**, 3017 (1994).

[10] D. R. Meacher, D. Boiron, H. Metcalf, C. Salomon, and G. Grynberg, Phys. Rev. A **50**, R1992 (1994).

[11] J. Guo and P. R. Berman, Phys. Rev. A **47**, 4128 (1993); J. Guo, *ibid.* **49**, 3934 (1994); **51**, 2338 (1995).

[12] B. Dubetsky and P. R. Berman, Phys. Rev. A **47**, 1294 (1993).

[13] R. Bonifacio and L. De Salvo, Nucl. Instrum. Methods Phys. Res. A **341**, 360 (1994); R. Bonifacio, L. De Salvo, L. M. Narducci, and E. J. D'Angelo, Phys. Rev. A **50**, 1716 (1994).

[14] See, for example, A. Aspect, E. Arimondo, R. Kaiser, N. Vansteenkiste, and C. Cohen-Tannoudji, J. Opt. Soc. Am. B **6**, 2112 (1989); M. Kasevich and S. Chu, Phys. Rev. Lett. **69**, 1741 (1992).

[15] A. Aspect, E. Arimondo, R. Kaiser, N. Vansteenkiste, and C. Cohen-Tannoudji, Phys. Rev. Lett. **61**, 826 (1988); M. Kasevich and S. Chu, *ibid.* **69**, 1741 (1992); J. Lawall, F. Bardou, B. Saubamea, K. Shimizu, M. Leduc, A. Aspect, and C. Cohen-Tannoudji, *ibid.* **73**, 1915 (1994).

[16] S. Stenholm, J. Phys. B **7**, 1235 (1974).

[17] P. R. Berman and R. Salomaa, Phys. Rev. A **25**, 2667 (1981).

[18] See, for example, P. R. Berman and W. E. Lamb, Jr., Phys. Rev. **187**, 221 (1969).

[19] P. R. Berman, Phys. Rep. **43**, 101 (1978); P. R. Berman and G. Grynberg, Phys. Rev. **39**, 570 (1989).

[20] For a "closed" system, in which $\Gamma_1\sim 0$ and spontaneous emission from level 2 to 1 at rate Γ_2 is included, the dressed-state population of level B is equal to θ^4 for $\theta\ll 1$ (see Ref. [17]). It is possible to simulate this result as well as others for a closed system by choosing a pumping rate proportional to θ^2. In this manner, the steady-state populations of the dressed states are comparable to those that would be obtained in a dressed-state model of a closed two-level system.

[21] The condition $\omega_k > 2\Gamma$ is necessary but not sufficient; in general, one must also have θ of order unity to ensure that the B resonances are not lost in the wings of the A resonances.

[22] B. Dubetsky and P. R. Berman, Phys. Rev. Lett. (to be published).

[23] For $p\neq 0$, terms ϵ_p, $\epsilon_p-2\hbar kv$ and $\epsilon_p+2\hbar kv$ should be added to the right-hand side of Eqs. (A1), (A2), and (A3), respectively, in addition to the replacements of Δ by $\tilde{\Delta}$ and δ by $\tilde{\delta}$.